Int. J. Impact Engng Vol.14, pp.145–156, 1993
Printed in Great Britain

0734-743X/93 $6.00+0.00
Pergamon Press Ltd

DESIGN AND PERFORMANCE EQUATIONS FOR ADVANCED METEOROID AND DEBRIS SHIELDS

ERIC L. CHRISTIANSEN

NASA Johnson Space Center, Mail Code SN3, Houston, Texas 77058

ABSTRACT

This paper provides equations defining the performance capability of various types of meteoroid and debris shielding systems. These equations have been developed at the NASA Johnson Space Center (JSC) Hypervelocity Impact Test Facility (HIT-F). Equations are included that are applicable for aluminum Whipple shields, Nextel® Multi-Shock (MS) shields, hybrid Nextel®/Aluminum MS shields, and Mesh Double-Bumper (MDB) shields. The MS and MDB shields are advanced shields with demonstrated weight and performance advantages over conventional Whipple shields.

NOMENCLATURE

C	Speed of sound in target (km/sec)
d	projectile diameter (cm)
d_c	critical projectile diameter (cm) causing failure
ρ	density (g/cm^3)
H	Brinell hardness of target (BHN)
m	areal density (g/cm^2)
M	projectile mass (g)
P	penetration depth (cm)
S	overall spacing between outer bumper and rear wall (cm)
σ	rear wall yield stress (ksi)
t	thickness (cm)
θ	impact angle (deg) measured from surface normal
V	projectile velocity (km/sec)
V_n	normal component of proj. velocity (km/sec) = V cos θ

Subscripts:

b	bumper(s) [all bumpers in Multi-Shock (MS) shield, first & second bumper in Mesh Double-Bumper (MDB) shield]
I	intermediate layer in MDB shield
p	projectile
t	target
w	rear wall
1,2,3,4	individual bumpers and spacings

INTRODUCTION

Research at the NASA Johnson Space Center (JSC) Hypervelocity Impact Test Facility (HIT-F) has resulted in a number of low-weight, state-of-the-art shielding concepts for spacecraft protection from meteoroid and orbital debris impact (Crews and Christiansen, 1992). One such concept, the Multi-Shock (MS) Shield, uses a spaced array of 4-5 thin sheets of aluminum, ceramic fabric or other materials to repeatedly shock and disintegrate impacting projectiles followed by a rear-wall to react the loading from the debris cloud (Cour-Palais and Crews, 1990). Another concept, the mesh double-bumper (MDB) consists of four elements: a mesh, a continuous aluminum sheet, high-strength fabric, and rear wall (Christiansen, 1990). Both the MS and MDB shields provide weight savings of approximately 50% at light gas gun velocities compared with conventional dual-sheet aluminum Whipple shields (Table 1). NASA is currently assessing the potential application of advanced shield concepts to Space Station *Freedom* (SSF), including hybrid forms of the MS and MDB shields that combine ceramic cloth and aluminum layers in various multi-bumper configurations to optimize performance capabilities within established design constraints. Results of HVI testing and performance assessments for one of many hybrid shield configurations under consideration are presented in this paper.

Table 1. Hypervelocity impact data for Whipple, Nextel® Multi-Shock (MS), and Mesh Double-Bumper (MDB) shields

Shield mass per unit area for no perforation or detached spall (All impacts at 6-7 km/sec)

Impact Angle	Overall Spacing (cm)	Shield Areal Density (g/cm^2) and (Test Number) Whipple	Multi-Shock	MDB
3.2 mm (45 mg) Aluminum Projectile				
0°	5	1.12 (JSC-A1464)	0.53 (JSC-A624)	0.41 (JSC-A963)
0°	10	0.60 (JSC-A235)	0.29 (JSC-A1231)	0.25 (JSC-A1285)
45°	10	1.50 (JSC-A1195)	0.31 (JSC-A1317)	0.36 (JSC-A1069)
6.4 mm (0.37 g) Aluminum Projectile				
0°	10	2.07 (JSC-B128)	1.10 (JSC-B112)	0.94 (JSC-B77)
0°	20	0.96 (JSC-B31)	0.63 (JSC-B70)	0.64 (JSC-B27)
9.5 mm (1.3 g) Aluminum Projectile				
0°	30	1.35 (ARC-1895)	1.02 (UDRI 4-1293)	1.08 (UDRI 4-1172)

For assessments of the vulnerability of spacecraft from meteoroids and debris, equations have been developed that define Whipple, MS, and MDB shield protection capabilities as a function of projectile diameter, velocity, impact angle, density, etc. These equations are updates of previous work (Cour-Palais, 1969; Cour-Palais and Crews, 1990; Christiansen, 1990). The shield performance equations are based on hypervelocity impact tests and analyses to cover the full range of expected on-orbit impact conditions. Orbital debris in low Earth orbit can impact at speeds exceeding 14 km/sec, with an average of ~10.3 km/sec. Meteoroids range from 11 to 72 km/sec. Most on-orbit impacts will be oblique, and only a fraction (<15% typically) will be within 10° to 20° of perpendicular (i.e., normal) to the spacecraft surface. Impact tests are used to derive the penetration equations up to the highest velocity attainable in the laboratory, and analytical/numerical techniques are used to determine shield response beyond test capabilities. Impact data to validate the equations is limited by light gas gun performance to approximately 8 km/sec. NASA has been actively supporting launcher development to extend the database to 10-12 km/sec.

The equations in this paper are presented in two parts: (1) sizing equations to determine preliminary estimates of shielding thicknesses and weights, and (2) performance (or "ballistic limit") equations to define the impact conditions, such as projectile size, velocity, density, and impact angle, that define the

maximum protection capability for a particular shield. The penetration or ballistic limit equations given in this paper are based on a failure criteria defined as perforation or detached spall of the rear wall of the shield. Other ballistic limit curves could be developed based on other failure modes. The ballistic limit equations are used in computer programs to calculate probabilities of damage from meteoroid and debris impacts (Christiansen and Hyde, 1992). These equations continue to be updated periodically as warranted by the results of additional hypervelocity impact (HVI) tests, analyses, and impact modelling.

SINGLE SHEET PROTECTION

In some cases, spacecraft components (such as electronic boxes, etc.) are "protected" by a single, monolithic material. To assess protection capabilities for single-sheet aluminum alloy "shields", penetration and perforation threshold equations were developed by Cour-Palais (1985, 1987). For projectile density ($\rho_p/\rho_t < 1.5$), the penetration depth into a semi-infinite target is:

$$P_\infty = 5.24\, d^{19/18}\, H^{-0.25}\, (\rho_p/\rho_t)^{0.5}\, (V_n/C)^{2/3} \tag{1a}$$

For projectile density ($\rho_p/\rho_t \geq 1.5$):

$$P_\infty = 5.24\, d^{19/18}\, H^{-0.25}\, (\rho_p/\rho_t)^{2/3}\, (V_n/C)^{2/3} \tag{1b}$$

If there is attached spall, the penetration depth is greater than into a semi-infinite target:

$$P = 1.05\, P_\infty \tag{2}$$

If there is detached spall, penetration depth can vary between 1.08 and 1.5 times the semi-infinite target penetration, that is

$$P = 1.08\, P_\infty \text{ to } 1.5\, P_\infty \tag{3}$$

The plate thickness to prevent perforation, but not detached spall is approximately 1.8 times the semi-infinite target penetration (this includes the detached spall thickness):

$$t = 1.8\, P_\infty \tag{4}$$

Plate thickness to prevent perforation and detached spall, but would allow attached spall is

$$t = 2.2\, P_\infty \tag{5}$$

Plate thickness to prevent perforation and incipient spall is

$$t = 3\, P_\infty \tag{6}$$

EQUATIONS FOR PRELIMINARY SHIELDING DESIGN

A simplified method is sometimes used (Cour-Palais, 1979; Christiansen, 1992) to roughly size the thicknesses of the bumper(s) and rear wall of meteoroid/debris shields and estimate shielding weights. A "design" particle size is calculated for each surface of a critical element from probability of no-failure requirements, environment models, surface area, and orientation considerations. Thicknesses and spacings for the various shield layers are then determined based on defeating the "design" particle at its average impact velocity, density, and impact angle. Although adequate for developing estimates of shielding weights and for performing quick trade studies, a more comprehensive approach is used for verifying design adequacy by considering the complete meteoroid/debris impact angle and velocity distributions.

EQUATIONS FOR PROBABILITY ANALYSES

Shielding protection capability is assessed by probability analyses which account for the directional nature of orbital debris and meteoroids, the complex response of the shielding to oblique and low speed

impact, and shadowing from nearby equipment (Christiansen et al., 1992; Crews and Christiansen, 1992).

The ballistic limit equations for Whipple, Multi-Shock (MS), and Mesh Double-Bumper (MDB) shields are in a form that relates critical particle diameter (d_c) with impact velocity, impact angle, particle density, and target parameters. Impacts larger than the critical particle size cause shield failure (i.e., perforation or detached spall of the rear wall of the hybrid shield), while those smaller do not. The equations are consistent with the equations given for shield sizing purposes, although additional equations are given to cover the full range of on-orbit impact velocities and impact angles.

DERIVATION OF EQUATIONS

The shielding equations in this paper are based on a number of HVI tests performed in the JSC Hypervelocity Impact Test Facility (HIT-F) and other facilities. The damage classification system of Dahl and Cour-Palais (1991) was used to standardize the shield damage observed in these hypervelocity impact tests. The criteria for shielding success in these tests was no perforation or detached spall from the in-board wall (or "rear wall") of the shield protection system. Over 200 tests on Whipple shields and 150 tests on Multi-Shock and Mesh Double-Bumper shields provide the basis of the performance equations. The tests used spherical projectiles up to ~8 km/sec. The velocity in the databases is limited by the capability of two-stage light gas guns, the workhorses of hypervelocity impact research. Although velocities less than 8 km/sec represent only ~25% of the debris threat, the HVI data includes the more damaging low velocity impacts for these particular shields (typically 2-3 km/sec) and therefore represents a higher percentage of the penetrating flux (Christiansen et al., 1992). In addition, the JSC HIT-F is currently evaluating data provided from a new generation of launchers such as an inhibited shaped charge launcher developed by Southwest Research Institute for NASA (Tullos et al., 1990) and Sandia National Laboratories' Hypervelocity Launcher (Chhabildis, 1992). Although these launchers can fire aluminum particles in excess of 10 km/sec, test analysis is complicated by the fact that the projectiles are non-spherical and subject to variations in impact orientation, size and shape. A primary use for the advanced launchers is for comparison with hydrocode results and calibration of the material models used in hydrocodes. The hydrocodes are then used to predict shield performance for >10 km/sec spherical particle impacts.

The equations for application beyond test capabilities have built on formulations originally developed for Whipple shields in the 1960's and 1970's which have been applied in evaluating meteoroid threats (Cour-Palais, 1969), as well as previously developed MS and MDB equations (Cour-Palais and Crews, 1990; Christiansen, 1990). Generally, a simple analytical relationship forms the basis of scaling to velocities beyond 8 km/sec, although JSC HIT-F applies more sophisticated analysis techniques such as hydrodynamic computer codes to evaluate the velocity scaling relations (Crews and Christiansen, 1992). These evaluations are still in progress.

ALUMINUM WHIPPLE SHIELDS

Figure 1 illustrates the Whipple shield concept which consists of a front bumper at some stand-off distance from a rear wall. The following equations are based on aluminum alloy shielding materials. Bumper and rear wall thicknesses for defeating a given particle threat can be determined by the following equations:

$$t_b = c_b\, m_p/\rho_b = c_b\, d\, \rho_p/\rho_b \tag{7}$$

$$t_w = c_w\, d^{0.5}\, (\rho_p\, \rho_b)^{1/6}\, M^{1/3}\, V_n/S^{0.5}\, (70/\sigma)^{0.5} \tag{8}$$

For aluminum on aluminum impacts (i.e., $\rho_p = \rho_b$), $c_b = 0.25$ when $S/d<30$ and $c_b = 0.20$ when $S/d\geq30$. In equation (8), $c_w = 0.16$ cm^2-sec/g$^{2/3}$-km. The coefficient c_b is increased to 0.25 to reduce the possibility of underestimating the required rear wall thickness with small standoff distances. These equations are based on a ballistic limit criterion defined as no perforation or detached spall of the rear wall of the shield.

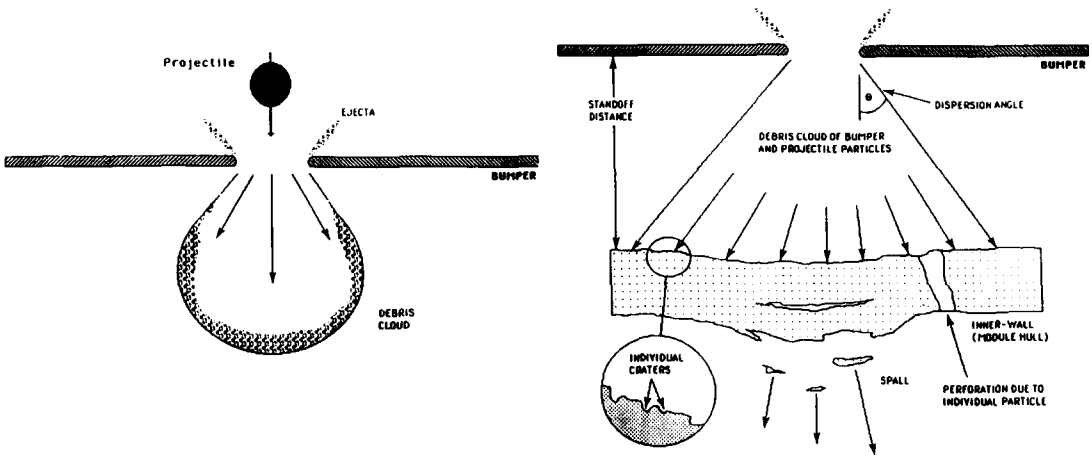

Figure 1. Whipple Shield (after Rajendran and Elfer, 1989)

Equation (8) is valid for particles impacting at a normal component velocity (V_n) of greater than 7 km/sec. The rear wall thickness relation is a slightly modified version of the Cour-Palais Whipple equation ("non-optimum") which was used in the Apollo program to extrapolate test data to meteoroid impact conditions (Cour-Palais, 1969). Coefficient c_w was derived from HVI testing with aluminum, glass, and nylon projectiles that varied in diameter from 0.04 cm to 1.9 cm (Christiansen, 1991b). If the S/d ratio is less than 15 for aluminum on aluminum impacts ($\rho_p = \rho_b$), or $(t_b \rho_b)/(d \rho_p)$ is less than 0.18 for normal impacts (not oblique) with V>7 km/sec, equation (8) potentially underpredicts rear wall thickness. Bumper fragments become the primary source of rear wall damage at impact angles greater than 65°. Therefore, above 65°, the calculated rear wall thickness should be constrained to 65°. More information on the derivation and applicability of these equations is contained elsewhere (Christiansen, 1991a; Cour-Palais, 1969).

The following equations define the protection capability limits for a Whipple shield in terms of a critical particle size (d_c) that causes shield failure (complete penetration or detached spall). Three penetration regimes are defined based on normal component velocity. At low velocities, below 3 km/sec, impact shock pressures are low and the projectile remains essentially intact after impact on the bumper. The shield's rear wall is then impacted by a deformed but substantially intact projectile. The critical particle size for $V_n \leq 3$ km/sec is given by

$$d_c = [(t_w (\sigma/40)^{0.5} + t_b)/(0.6 (\cos \theta)^{5/3} \rho_p^{0.5} V^{2/3})]^{(18/19)} \quad (9)$$

The projectile is more damaging as velocity increases in the low velocity regime, thus critical particle size decreases as velocity increases. At velocities above V_n=3 km/sec, the projectile fragments on the bumper and will begin to melt above V_n = ~5.5 km/sec for aluminum on aluminum impacts (Swift, 1982). A fragmenting or partially molten projectile is less damaging to the rear wall, thus critical particle size increases in the intermediate velocity range.

For 3 km/sec < V_n < 7 km/sec:

$$d_c = \{[(t_w (\sigma/40)^{0.5} + t_b)/(1.248 \rho_p^{0.5} \cos \theta)]^{(18/19)} \times$$

$$(1.75 - (V \cos \theta)/4)\} + \{[1.071 t_w^{2/3} \rho_p^{-1/3} \rho_b^{-1/9} S^{1/3} (\sigma/70)^{1/3}] \times$$

$$((V \cos \theta)/4 - 0.75)\} \quad (10)$$

At velocities above 7 km/sec, the debris cloud impacting the rear wall will contain various fractions of solid, liquid, and vapor components of the projectile and bumper depending on impact conditions (projectile shape, obliquity, density, etc.). For $V_n \geq 7$ km/sec, critical particle size is given by

$$d_c = 3.918\, t_w^{2/3}\, \rho_p^{-1/3}\, \rho_b^{-1/9}\, (V \cos\theta)^{-2/3}\, S^{1/3}\, (\sigma/70)^{1/3} \qquad (11)$$

For oblique impact angles over 65°, critical particle sizes should be set to the critical particle sizes for 65° impact, because of the increased damage to the rear wall from bumper fragments; i.e.,

$$d_c^{\theta>65} = d_c^{\theta=65} \qquad (12)$$

An example of set of ballistic limit curves for a 10 cm standoff Whipple shield (1.25 g/cm^2 total areal density) is shown in Figure 2. The plot is of particle diameter to fail the shield as a function of impact speed for different impact angles (failure of the shield occurs above the curves). This shows low speed (~2-3 km/sec) and higher speed (~7 km/sec) oblique impacts can be more damaging (i.e., they have lower critical diameters) than higher speed (~7 km/sec) normal impacts. A key factor governing the performance of Whipple shields is the "state" of the debris cloud projected from the bumper toward the rear wall. Whipple shields are less effective at low impact velocities and certain oblique impact angles at higher speeds because these are the conditions which generate low impact pressures in the projectile and bumper that result in solid, more penetrating fragments impacting the rear wall.

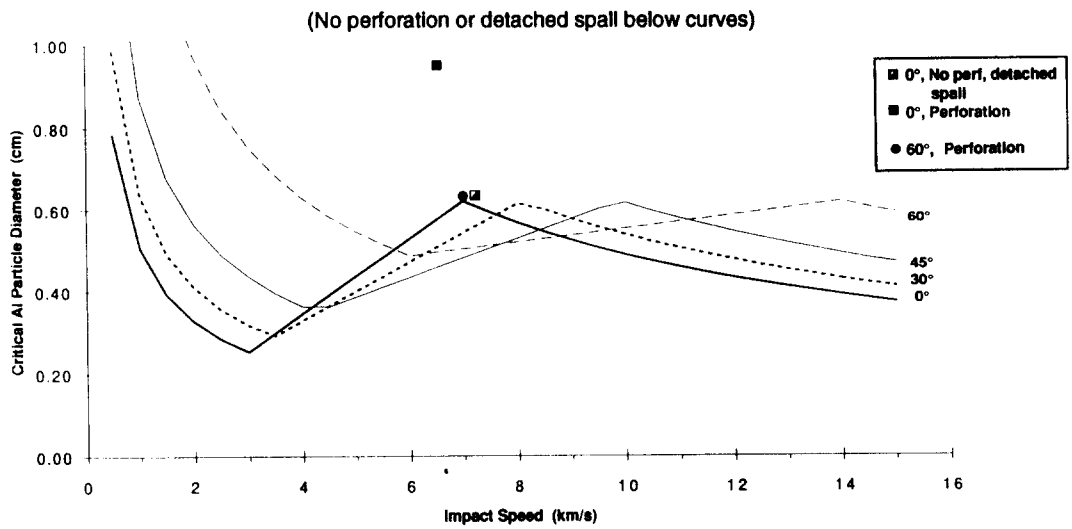

Figure 2. Whipple Shield Ballistic Limit Curves: 0.127 cm Al 6061-T6 bumper, 10.2 cm spacing, 0.32 cm Al 2219-T87 rear wall, total shield areal density = 1.25 g/cm^2

NEXTEL MULTI-SHOCK (MS) SHIELD

The multi-shock (MS) shield (Figure 3) is a low-weight shielding alternative to the Whipple shield. Sizing equations for two types of MS shield are given below: (1) Four equally spaced ceramic fabric bumpers with an aluminum rear wall, and (2) An all-flexible shield consisting of four equally spaced ceramic fabric bumpers with a ceramic fabric rear wall. A ceramic fabric that has been tested extensively at the JSC HIT-F is Nextel®, an alumina, boron oxide, silica ceramic product made by 3M Corporation. In these equations, the combined areal density of all four Nextel® bumpers is given by "m_b", and the overall spacing (from outermost bumper to the rear wall) is given by "S". The areal density of all four MS bumpers is approximately equal to the areal density of the single bumper in a Whipple shield. Major weight savings occur in reducing the rear wall thickness required to stop a given threat particle.

For MS ceramic fabric bumpers and aluminum wall:

$$m_b = 0.19\, m_p = 0.19\, d\, \rho_p \qquad (13)$$

$$m_w = 41.7\, M\, V_n/S^2\, (40/\sigma)^{0.5} \quad (14)$$

For MS ceramic fabric bumpers and ceramic fabric wall:

$$m_b = 0.19\, m_p = 0.19\, d\, \rho_p \quad (15)$$

$$m_w = 43.6\, M\, V_n/S^2 \quad (16)$$

These equations are slightly modified version from the MS equations presented by Cour-Palais and Crews (1990). The wall areal densities calculated by Equations 14 and 16 are based on the ballistic limit criteria of preventing perforation and detached spall. HVI testing with aluminum projectiles up to 1 cm have been performed on the Nextel® bumper and aluminum wall MS configuration. These equations can be applied for a component velocity ($V \times \cos^{0.25}\theta$) of greater than 6.4 km/sec and S/d ratio of greater than 15. These equations are valid for all impact angles.

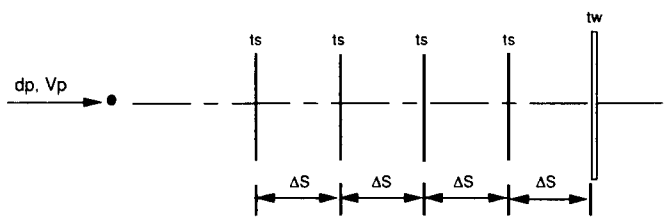

- Multiple, ultra-thin, spaced sheets (TS/DP <03)
- Successive shocks raise thermal state of projectile
- Flexible or rigid shields materials
- Flexible material: ceramic fabric
  - Nextel (3M brand name): 62% Al2O3, 24 SiO2, 14% B2O3
  - Versatile. Many on-orbit augmentation options.
- Augmentation shield using deployable concepts.

Figure 3. Multi-Shock Shield (Cour-Palais and Crews, 1990)

No limits are necessary on oblique impacts because the ceramic fabric bumpers do not produce damaging fragments. Particles produced by impacts on the ceramic fabrics are short fibers up to several millimeters long but only 10-12 microns in diameter. Nextel® bumper particles ejected normal to the bumper during oblique impact generally do not penetrate subsequent bumper layers and therefore do not damage the rear wall. Bumper fragments from a Whipple shield are far more damaging to the rear wall for two reasons: (1) an oblique impact on the bumper of the Whipple shield (which is ~4 times heavier than a MS bumper) produces bumper fragments that are larger and more penetrating than the tiny fiber particles from a MS fabric bumper and (2) these bumper particles impinge directly on the rear wall of the Whipple shield in contrast with the MS shield where bumper particles are stopped by lower layers of the MS shield before reaching the rear wall.

The following MS shield ballistic limit equations are valid for a shield consisting of 4 Nextel® bumpers and an aluminum rear wall, with equal spacing between sheets. In these equations, the overall spacing from the first, outer-most, bumper to the rear wall is given by "S".

For $V \geq 6.4/(\cos\theta)^{0.25}$:

$$d_c = 0.358\, (t_w\, \rho_w)^{1/3}\, \rho_p^{-1/3}\, V^{-1/3}\, (\cos\theta)^{-1/3}\, S^{2/3}\, (\sigma/40)^{1/6} \quad (17)$$

For $2.4/(\cos\theta)^{0.5} < V < 6.4/(\cos\theta)^{0.25}$:

$$d_c = 1.12\, \rho_p^{-0.5}\, [t_w\, (\sigma/40)^{0.5} + 0.37\, m_b]\, (\cos\theta)^{-1}$$

$$[(6.4/(\cos\theta)^{0.25} - V)/(6.4/(\cos\theta)^{0.25} - 2.4/(\cos\theta)^{0.5})]$$

$$+ 0.193\, (t_w\, \rho_w)^{1/3}\, \rho_p^{-1/3}\, (\cos\theta)^{-1/4}\, S^{2/3}\, (\sigma/40)^{1/6}$$

$$[(V - 2.4/(\cos\theta)^{0.5})/(6.4/(\cos\theta)^{0.25} - 2.4/(\cos\theta)^{0.5})] \quad (18)$$

For $V \leq 2.4/(\cos\theta)^{0.5}$:

$$d_c = 2\,[t_w\,(\sigma/40)^{0.5} + 0.37\,m_b]/[(\cos\theta)^{4/3}\,\rho_p^{0.5}\,V^{2/3}] \quad (19)$$

Figure 4 illustrates the results of applying the above equations for a small-scale MS shield (0.31 g/cm^2 shield areal density, 10 cm overall spacing). This plot shows that a 3.2 mm aluminum projectile impacting at 6.5 km/sec and normal impact angle will be on the ballistic limit of the shield, while the shield will stop a 1.25 mm projectile in a normal impact at 3 km/sec.

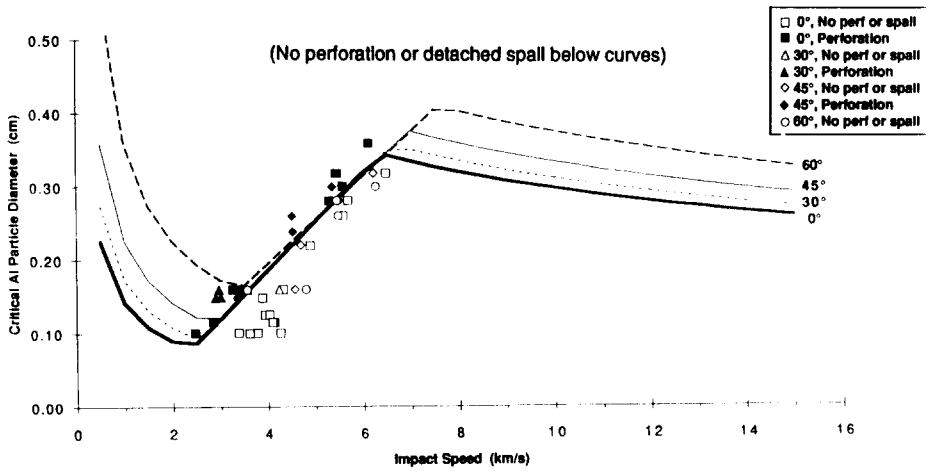

Figure 4. Multi-Shock Shield Ballistic Limit Curves: MS consists of four Nextel® AF26 bumpers (0.043 g/cm^2 each) and a 0.0508 cm Al 2024-T3 rear wall, with 2.54 cm between each sheet, 10.16 cm overall spacing, 0.31 g/cm^2 total

MESH DOUBLE-BUMPER (MDB) SHIELD

The Mesh Double-Bumper (MDB) is another advanced shield that provides similar protection and weight savings benefits as the MS shield. A schematic of the MDB shield is given in Figure 5. It was developed to show major improvements in the shielding protection capability of a Whipple shield could be made simply by adding a mesh a short distance in front of the Whipple bumper and putting a high-strength fabric layer (Kevlar®, Spectra®, or ceramic cloth) between the Whipple bumper and rear wall. Impact testing at the JSC HIT-F has shown that a double bumper system with a mesh outer bumper exhibits superior performance than the same weight double bumper consisting of two continuous aluminum sheets. Equations for sizing MDB shields and predicting performance are given by Christiansen and Kerr (1992).

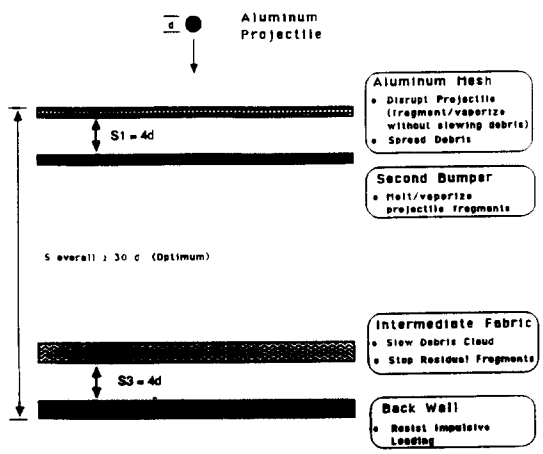

- Aluminum mesh:
  - Mass efficient method to disrupt projectile
  - Greater spread of debris cloud results from impacts on mesh; reduces performance degradation at smaller spacings.
  - Fine mesh used. Small projectiles passing unhindered through mesh easily defeated by remaining shield elements.
  - Improvement over equal-weight aluminum double bumpers.
- Second bumper used to deliver second shock to remaining fragments.
- Intermediate layer of high-strength fabric (Spectra, Kevlar, Nextel, etc.) used to decrease impulsive loading on back sheet.

Figure 5. Mesh Double-Bumper Shield (Christiansen, 1990)

HYBRID NEXTEL/ALUMINUM MULTI-SHOCK SHIELDS

Hybrid MS shields are defined as a MS combination of Nextel® and aluminum bumpers and aluminum rear wall. Hybridized MS (and MDB) shields are being considered for application on SSF because it is relatively uncomplicated to improve the protection capability of certain Whipple shields by adding 2 to 3 Nextel® layers in the hybrid shield configuration (i.e., over the Whipple shield). The hybrid shield considered in this section is a triple-bumper shield containing two layers of Nextel® ceramic cloth over an aluminum 2-sheet Whipple shield (Figure 6). The 2 outer Nextel® bumpers and the aluminum bumper are all equally spaced from each other. The spacing between the aluminum bumper and aluminum rear wall is twice the inter-bumper spacing. Both Nextel® sheets together contain approximately the same areal density as the aluminum bumper, while the rear wall is approximately twice the areal density of the aluminum bumper. HVI testing investigated a range of different hybrid MS shields, including:

(1) A 20 cm overall standoff (1.05 g/cm^2) hybrid shield (100% scale model) with 2 Nextel® BF54 bumpers (0.108 g/cm^2 each), a 0.1 cm Al 6061-T6 bumper, and a 0.18 cm Al 6061-T6 rear wall.

(2) A 40% model of the hybrid shield in (1): A 7.6 cm overall standoff (0.42 g/cm^2) hybrid shield with 2 Nextel® AF26 bumpers (0.043 g/cm^2 each), a 0.041 cm Al 6061-T6 bumper, and a 0.081 cm Al 6061-T6 rear wall.

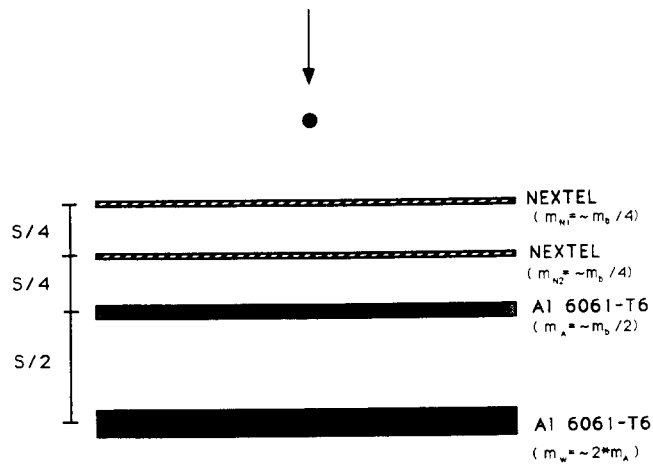

Figure 6. Hybrid Nextel®/Aluminum Multishock Shield

Ballistic limit equations for the hybrid shield are given below based on analysis of the ~50 HVI tests completed at the JSC HIT-F on hybrid shields. The impact tests demonstrated dimensional scaling over target sizes varied by 2.5 times (i.e., a 40% scale model that defeats a 2.5 mm particle was scaled to a 100% model that defeats a 6.3 mm particle).

For $V \geq 6.5/(\cos\theta)^{2/3}$:

$$d_c = 2.4\,(t_w\,\rho_w)^{2/3}\,\rho_p^{-1/3}\,\rho_A^{-1/9}\,(V\cos\theta)^{-2/3}\,S^{1/3}\,(\sigma/40)^{1/3} \qquad (20)$$

For $2.7/(\cos\theta)^{0.5} < V < 6.5/(\cos\theta)^{2/3}$:

$$d_c = 1.031\,\rho_p^{-0.5}\,[t_w\,(\sigma/40)^{0.5} + 0.37\,m_b]\,(\cos\theta)^{(1/3-x)}$$

$$[(6.5/(\cos\theta)^{2/3} - V)/(6.5/(\cos\theta)^{2/3} - 2.7/(\cos\theta)^{0.5})]$$

$$+ 0.689\,(t_w\,\rho_w)^{2/3}\,\rho_p^{-1/3}\,\rho_A^{-1/9}\,(\cos\theta)^{-2/9}\,S^{1/3}\,(\sigma/40)^{1/3}$$

$$[(V - 2.7/(\cos\theta)^{0.5})/(6.5/(\cos\theta)^{2/3} - 2.7/(\cos\theta)^{0.5})] \qquad (21)$$

For $V \leq 2.7/(\cos\theta)^{0.5}$:

$$d_c = 2\,[t_w\,(\sigma/40)^{0.5} + 0.37\,m_b]/[(\cos\theta)^x\,\rho_p^{0.5}\,V^{2/3}] \quad (22)$$

where,

$x = 7/3$ when $\theta \leq 45°$

$x = 2$ when $\theta > 45°$

$m_b = m_N + t_A\,\rho_A$ (N = Nextel bumpers, A = Aluminum bumper)

For oblique impact angles over 75°, use the d_c calculated at 75°; i.e., for $\theta > 75°$:

$d_c^{\theta>75} = d_c^{\theta=75}$

Figure 7 shows the ballistic limit curves for a hybrid shield with the same layup as the 40% scale model (i.e., the second configuration discussed above).

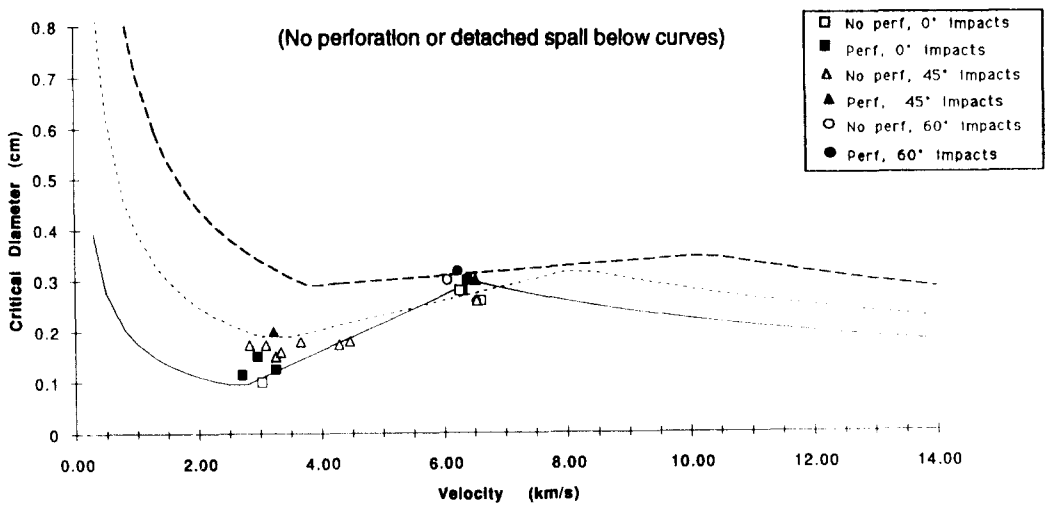

Figure 7. Hybrid Nextel®/Aluminum MS Ballistic Limit Curves: Two Nextel® AF26 bumpers (0.043 g/cm^2 each), 1.9 cm between bumpers, 0.041 cm Al 6061T6 third bumper, 3.8 cm spacing, 0.08 cm Al 6061T6 rear wall, 7.6 cm overall spacing, 0.42 g/cm^2 total

SUMMARY OF ADVANTAGES FOR MULTI-BUMPER SHIELDS

Besides improved performance, multi-bumper shields (such as the MS, MDB, and hybrid MS shields) offer a number of advantages over conventional Whipple shields that are not completely evident from the performance and design equations given above, including:

(1) *Less damaging external secondary debris (ejecta)*: The thin Nextel® bumpers in MS shields, and mesh bumpers in MDB shields, generate less external secondary ejecta in oblique impacts. The secondaries that are produced are fine grained and result in little damage into witness plates compared to Whipple shields.

(2) *More efficient at converting projectile's initial kinetic energy to internal thermal energy*: Alme et al. (1991) has demonstrated by numerical simulation that a series of shocks produced by multi-bumper shields increases the heating of the projectile compared to the single shock provided in impacts with the bumper of a Whipple shield.

(3) *Less sensitive to projectile shape*: Multi-bumper shields are less prone to perforation by disks, cylinders and other non-spherical projectiles than Whipple shields because the multiple shocks disrupt

the projectile to a greater extent. Numerical simulations at the JSC HIT-F and by Williamsen and Tipton (1990) support this conclusion.

(4) *Less sensitive to oblique impacts*: HVI tests and the equations in this paper indicate that oblique impacts can be more damaging on Whipple shields than multi-bumper shields. Multiple shocks from multiple bumpers cause greater projectile fragmentation and heating than a single bumper Whipple shield, which suffers from less projectile fragmentation in oblique impacts (up to 60°) in the 4-8 km/sec range. Also, multi-bumper systems have several layers that slow the expansion of the debris cloud before it collides with the rear wall, whereas the Whipple shield has no intervening bumpers to slow debris cloud expansion (Boslough et al., 1992). This reduction in the debris cloud expansion speed is even more pronounced in oblique impacts on multi-bumper systems, because of the greater spread and increased bumper contact area as impact obliquity angle increases.

(5) *Less cumulative damage to the shield's rear wall*: Over time, bumper fragments from numerous small strikes will crater and damage the rear wall of a Whipple shield more often than multi-bumper systems. The outer bumpers of the Whipple and multi-bumper shields will be perforated and spalled by relatively small particles. In multi-bumper shields, the intermediate layers of the shield stop bumper fragments from impacting and damaging the rear wall; whereas, the Whipple shield has no such protection. This can be a maintenance/inspection consideration for long duration spacecraft.

CONCLUSIONS

This paper gives sizing and ballistic limit equations that are applicable for a variety of spacecraft materials and shielding systems. Data and analyses supporting these equations were discussed (also see references to Christiansen, Cour-Palais and Crews). Tests and analyses on these and other promising shielding systems are continuing at the JSC Hypervelocity Impact Test Facility (HIT-F) and these equations will continue to evolve.

ACKNOWLEDGEMENTS

The author appreciates the many contributions to this work from Jeanne Lee Crews, Manager of the NASA JSC Hypervelocity Impact Research Laboratory (HIRL), and Burton G. Cour-Palais, McDonnell Douglas Space Systems Company. The excellent support from HIT-F personnel, including Lu Borrego, Earl Brownfield, Ed Cykowski, Joe Falcon, Jim Hyde, Jay Laughman, Javier Ortega, Ken Oser, Pat White, and Jim Whitney, is also appreciated.

REFERENCES

Alme, M.L., Christiansen, E.L., and Cour-Palais, B.G. (1991). Hydrocode Simulations of the Multi-Shock Meteoroid and Debris Shield. Proceedings of the APS 1991 Topical Conference on Shock Compression on Condensed Matter, Williamsburg, VA, June 17-20, 1991.

Boslough, M.B., Ang, J.A., Chhabildas, L.C., Cour-Palais, B.G., Christiansen, E.L., and Crews, J.L. (1992). Hypervelocity Testing of Advanced Shielding for Spacecraft Against Impacts to 10 km/s. *Int. J. Impact Engng*, to be published.

Chhablidis, L. (1992). A New Hypervelocity Launcher (HVL) for Space Science Application. AIAA Paper Number 92-1639.

Christiansen, E.L. (1990). Advanced Meteoroid and Debris Shielding Concepts. AIAA Paper No. 90-1336, presented at AIAA/NASA/DOD Orbital Debris Conference, Baltimore, MD, April 16-19, 1990.

Christiansen, E.L. (1991a). Whipple Shield Sizing Equations. NASA JSC Memorandum SN3-91-19, March 1, 1991. NASA TM-105539.

Christiansen, E.L. (1991b). Whipple, Multi-Shock, and Mesh Double- Bumper Shield Hypervelocity Impact Data. NASA JSC Memorandum SN3- 91-95, June 19, 1991. NASA Technical Memorandum to be published.

Christiansen, E.L. (1992). Performance Equations for Advanced Orbital Debris Shields. AIAA Paper No. 92-1462, presented at the AAIA Space Programs and Technologies Conference, Huntsville, AL, March 24-27, 1992.

Christiansen, E.L., Hyde, J. and Snell, G. (1992). Spacecraft Survivability in the Meteoroid and Debris Environment. AIAA Paper Number 92-1409.

Christiansen, E.L. and Kerr, J.H. (1992). Mesh Double-Bumper Shield: A Low-Weight Alternative for Spacecraft Meteoroid and Orbital Debris Protection. *Int. J. Impact Engng*, to be published.

Cour-Palais, B.G. (1969). Meteoroid Protection by Multi-Wall Structures. AIAA Hypervelocity Impact Conference, AIAA Paper Number 69-372.

Cour-Palais, B.G. (1979). Space Vehicle Meteoroid Shielding Design. ESA SP-153, pp.85-92.

Cour-Palais, B.G. (1985). Hypervelocity Impact Investigations and Meteoroid Shielding Experience Related to Apollo and Skylab. NASA Conference Publication 2360, Orbital Debris, pp.247-275.

Cour-Palais, B.G. (1987). Hypervelocity Impact in Metals, Glass and Composites. *Int. J. Impact Engng* Vol.5, pp.221-237.

Cour-Palais, B.G. and Crews, J.L. (1990). A Multi-Shock Concept for Spacecraft Shielding. *International Journal of Impact Engineering*, Vol.10, pp.135-146.

Crews, J.L. and Christiansen, E.L. (1992). NASA Johnson Space Center Hypervelocity Impact Test Facility (HIT-F). AIAA Paper Number 92-1640.

Dahl, K.V. and Cour-Palais, B.G. (1991). Standardization of Impact Damage Classification and Measurements for Metallic Targets. To be published at the 1992 Hypervelocity Impact Symposium.

Rajendran, A.M. and Elfer, N. (1989). Debris Impact Protection of Space Structures. In: *Structural Failure* (Wierzbicki, ed.), John Wiley & Sons.

Swift, H.F. (1982). Hypervelocity Impact Mechanics. In: *Impact Dynamics* (Zukas, ed.), John Wiley & Sons.

Tullos, R., Grosch, D., and Walker, J. (1990). An Explosive Hypervelocity Launcher for Orbital Debris Impact Simulations at 11.4-11.9 km/s. Southwest Research Institute, Report 06-2880, San Antonio, TX.

Williamsen, J.E. and Tipton, J.P. (1990). *Freedom* Station Wall Design Using Hydrodynamic Modelling. AIAA Paper No. 90-3664.